

Photoluminescence Spectroscopy of Band Gap Shrinkage in GaN

Niladri Sarkar and Subhasis Ghosh

School of Physical Sciences, Jawaharlal Nehru University, New Delhi 110067

We present an experimental investigation of band-gap shrinkage in n-type GaN using photoluminescence spectroscopy, as a function of electron concentration and temperature. The observed systematic shift of the band-to-band transition energy to lower energies with increasing electron concentration has been interpreted as many-body effects due to exchange and correlation among majority and minority carriers. The band-to-band transition energy also shifts to lower energy with increasing temperature. The parameters that describe the temperature dependence red-shift of the band-edge transition energy are evaluated using different models and we find that the semi-empirical relation based on phonon-dispersion related spectral function leads to excellent fit to the experimental data.

PACS numbers: 78.20.-e, 78.55.-m, 78.55.Cr

In recent years, GaN and its ternary alloys have been extensively studied for their application in blue and ultra-violet light emitting devices, short wavelength lasers, and electronic devices for high power and high temperature applications¹. This tremendous application potential originates from the wide range of direct energy band gaps, the high breakdown voltage, and the high saturation electron drift velocity. In spite of technological breakthrough in GaN growth, doping and metal-GaN contacting technologies, several fundamental issues, such as temperature and doping induced band gap shrinkage(BGS) are still controversial. In particular BGS is extremely important for the development and modeling of GaN-based high temperature and high power devices. The effects of heavy doping on the optical and electrical properties of semiconductors have been widely investigated² over the years because of two reasons: first the fundamental physics underlying BGS and second their importance in device applications. Heavily doped layers are integrated in many devices and the estimation of BGS is an important input in device simulations. Furthermore, several theoretical calculations^{3,4,5,6} with different techniques have been published. Hence more experiments on BGS in different semiconductors with different intervals of doping would therefore appear motivated. The effect of doping on the band-to-band(BB) transition energy in heavily doped GaN has been studied by photoluminescence(PL) and photoreflectance(PR) spectroscopy by several groups^{7,8,9,10,11,12} and the value of the BGS coefficient obtained from $n^{1/3}$ power-law fit varies between -1.3×10^{-8} to $-4.7 \times 10^{-8} eVcm$ at room temperature, where n is the electron concentration. Moreover, all the previous studies^{7,8,9,10,11,12} on GaN have ignored the contribution of correlation term, which is proportional to $n^{1/4}$ in doping induced BGS. Recently, we have shown¹³ in detail the importance of this term on doping induced BGS in $Al_xGa_{1-x}As$.

The temperature induced BGS is observed in experiments by a monotonic red shift of either BB and/or excitonic transitions that are observed in bulk as well as low dimensional heterostructures. The temperature dependence of the band gap $E_g(T)$ varies from relatively weak in the low temperature region to relatively strong at higher temperature region. There is considerable controversy regarding the temperature induced BGS and linewidth broadening. All the previous studies^{14,15,16,17,18,19} on GaN have used empirical relations^{20,21} neglecting the role of phonon dispersion in GaN^{22,23} to explain the experimental data. There is large variation of the values of different BGS and linewidth broadening parameters, for example, in case of BGS, the most fundamental parameter α , which is $-dE_g(T)/dT$ at high temperature limit, varies from 0.36meV/K to 1.2meV/K in the literature^{14,15,16,17,18,19}. Pässler^{24,25} has shown the inadequacy of these empirical relations for temperature induced BGS in semiconductors, in particular the inapplicability²⁶ of these relations in case of wide band gap semiconductors. In addition, residual strain between GaN epilayers and substrates(sapphire and SiC) due to mismatch in lattice constant and thermal conductivity is also responsible for scattering in the values of different BGS parameters.

PL spectroscopy has emerged as a standard and powerful technique to study the optical properties of bulk and low-dimensional semiconductor structures. It is highly desirable to adopt a noncontact, nondestructive optical technique to determine the homogeneity of the crystalline quality and distribution of alloy composition in the epitaxial layer. PL spectroscopy is routinely used to characterize the quality of semiconductor substrates and thin epitaxial layers for different device structures. PL spectroscopy is a direct way to measure the band-gap energy as a function of different parameters, such as carrier concentration, excitation intensity, temperature, pressure, and magnetic field. The low-temperature PL spectra from III-V binary and ternary compound semiconductors with reasonably good crystalline quality are dominated by band-edge and near-band-edge transitions. The underlying recombination processes can be identified from the behavior of PL spectra as a function of temperature and excitation intensity. Low-temperature PL spectroscopy is usually performed to study the excitonic recombination mechanisms in semiconductors, but recently room-temperature PL spectroscopy has received attention for different reasons. In most cases, BB transitions can be observed only at room temperature or at higher temperature. Several many-body effects such as BGS, screening, and

carrier-exciton scattering can be studied using room-temperature PL spectroscopy. Beside the understanding of basic physics regarding the mechanism of recombination processes at higher temperature, determination of the quantum efficiency of the BB transition at room temperature is extremely important for optoelectronic devices.

In this work, we present the electron concentration and temperature dependence of BGS in GaN epilayers. In particular, the role of background electron concentration on the band gap and different parameters responsible for temperature induced BGS is studied. The results are compared with different empirical and semi-empirical models for BGS. Our samples are grown on c-plane sapphire substrates by metalorganic chemical-vapor deposition(MOCVD) in a vertical rf-heated, rotating disk quartz reactor at 76 Torr. Previous studies^{27,28} have shown that excess Ga in the buffer layer improves the crystal quality of GaN epilayers through strain relaxation and increased adatom surface mobility during the initial stage of epitaxial growth. We have recently shown²⁹ that conductivity and the defect-related optical properties of GaN epilayers can be significantly controlled by the III/V ratio in GaN buffer layer. Prior to the growth of the epilayers, a 30-nm-thick GaN buffer layer were grown at 565 C. After growing the buffer layer, the substrate temperature was raised to 1000 C for subsequent 1.6 μ m thick GaN epilayers. Five sets of samples were grown with different trimethylgallium(TMg) flow rates of 14, 24, 34, 48, and 55 mmol/min in the buffer layer, while keeping the flow rate of NH₃ and H₂ constant at 1.5 and 2.5 slm, respectively. The crystalline quality of the GaN epitaxial films was evaluated by x-ray double-crystal diffraction using GaN symmetrical(002) and asymmetrical(104) reflections. More details of the samples are given in Ref.29. The electron concentrations were measured by Hall measurements. The electron concentrations were determined by Hall measurements. We have chosen set of n-type samples with electron concentration in the range of 2.0×10^{16} to 2.7×10^{18} cm⁻³. The PL spectra were collected in the wavelength region of 340-900nm. The samples were kept in a closed cycle He refrigerator and were excited with 325nm laser line of He-Cd laser. The PL signal was collected into a monochromator and detected with a UV-enhanced Si detector.

Typical high temperature emission spectra in n-type GaN as a function of electron concentration are shown in Fig.1 and it is clear that BB peaks shift towards lower energy as the electron concentration increases. This is a direct evidence for the BB transition. Fig.1. also shows the PL spectra at 10K. The low temperature PL spectra show bound exciton(BE) at about 3.47eV and multiple peaks due to donor-acceptor pair(DAP) recombination^{29,30,31} at lower energies. We have avoided band-gap filling in our GaN samples by carefully choosing the carrier concentration such that except for the sample with carrier concentration 2.7×10^{18} cm⁻³, all samples are nondegenerate. It is clear in Fig.1 that BB peak is not broadened as the carrier concentration increases. The redshifts of BB transitions in GaN at 300K and 320K are shown in Fig.2.

In a heavily doped semiconductors, the density of states differs from that of the undoped pure crystal due to many-body effects. The presence of the large concentration of free carriers can cause a significant reduction of the unperturbed band gap in semiconductors. This reduction is caused by many-body effects and carrier-impurity interactions. As the doping density increases, the conduction band edge moves downward and the valence band edge moves upward. In addition to doping induced BGS, perturbation to the unperturbed band gap E_g^0 can come from (i) a random distribution of impurities which are almost independent of doping density³², and (ii) an interaction between electrons and donor impurities, which is appreciable only for very high carrier concentration($> 10^{19}$ cm⁻³)³². It is almost impossible to separate the cumulative contribution to BGS from various many-body interactions. We are only interested in the role of electron-electron interaction on band gap. To avoid contributions due to (i) and (ii), we have performed our BGS experiments with moderately doped samples with a maximum electron concentration of 10^{18} cm⁻³. The subject of this investigation is to study the effect of electron-electron interactions on BGS, which has been studied theoretically by several groups^{3,4,5,32} and the effective change in the band gap due to many-body interactions can be given by

$$\Delta E_g = -an^{1/3} - bn^{1/4} \quad (1)$$

where, a and b are BGS co-efficients. The first term is due to the exchange interaction, which comes from the spatial exclusion of the like spins away from each other. The second term is due to the correlation energy, which comes from the repulsion of the like charges, so that they do not move independently, but in such a way so as to avoid each other as far as possible. The values of co-efficients a and b are 1.5×10^{-8} eVcm and 3.0×10^{-9} eVcm^{3/4}, respectively, evaluated by fitting with experimental data, as shown in Fig.2.

Temperature dependence of the band-gap E_g of two n-type GaN samples with different background electron concentrations is shown in Fig.3 and 4, which shows a maximum redshift of about 65meV as temperature increases from 10K to 320K. An appropriate fitting function is required to obtain material-specific parameters from experimentally measured $E_g(T)$. There are two set of fitting function for $E_g(T)$ in the literature: (i) empirical relations proposed by Varshni²⁰ and Viña et al²¹ and (ii) semi-empirical relations based on the electron-phonon spectral function $f(\epsilon)$ and the phonon occupation number $n(T)$, ϵ is the phonon energy.

The most frequently used empirical relation for numerical fittings of $E_g(T)$ was first suggested by Varshni²⁰ and given by

$$E_g(T) = E_g(0) - \frac{\alpha T^2}{\beta + T} \quad (2)$$

where $E_g(0)$ is the band gap at 0K, α is the $T \rightarrow \infty$ limiting value of the BGS coefficient $dE_g(T)/dT$ and β is a material specific parameter. This model represents a combination of a linear high-temperature dependence with a quadratic low-temperature asymptote for $E_g(T)$. Though this phenomenological model gave reasonable fittings of $E_g(T)$ in elemental, III-V and II-VI semiconductors with $E_g \leq 2.5\text{eV}$, there have been several problems with this relation, for example, (i) this relation gives negative values of α and β in case of wide band gap semiconductors^{20,26}, (ii) β is a physically undefinable parameter believed to be related to Debye temperature Θ_D of the semiconductor, but this connection has been doubted strongly in several cases²⁵ and (iii) it has been shown that this relation cannot describe the experimental data of $E_g(T)$ even in GaAs³³. Fig.3(a) and 4(a) show the comparison of experimental $E_g(T)$ with Varshni's relation²⁰. We have obtained the values of α in the range of 0.54 meV/K to 0.63 meV/K and β in the range of 700 K to 745K for the samples with electron concentrations of 9.8×10^{16} to $2.7 \times 10^{18} \text{ cm}^{-3}$. The parameter β in this model only gives an estimation of Θ_D , which is about 870K in GaN. It is clear that though the fitting is good in the low temperature region ($< 100\text{K}$), but fitting is poor in the intermediate ($\sim 100\text{K}$) and high temperature region ($> 200\text{K}$).

Viña et al²¹ first emphasized that total BGS, $\Delta E_g(T) = E_g(0) - E_g(T)$ is proportional to average phonon occupation numbers $\bar{n}(T) = \left[\exp\left(\frac{\epsilon}{k_B T}\right) - 1 \right]^{-1}$ and proposed an empirical relation, which can be expressed as

$$E_g(T) = E_g(0) - \frac{\alpha_B \Theta_B}{\exp\left(\frac{\Theta_B}{T}\right) - 1} \quad (3)$$

where $\alpha_B = \frac{2a_B}{\Theta_B}$, a_B is a material parameters related to electron-phonon interaction, $\Theta_B = \frac{\hbar\omega_{eff}}{k_B}$ represents some effective phonon temperature and ω_{eff} is the effective phonon frequency. Though this phenomenological model gave reasonable fittings of $E_g(T)$ in different semiconductors, there are also several problems with this relation, for example, (i) at low temperature, this model shows a plateau behavior of $E_g(T)$, which is not observed experimentally, (ii) at higher temperature ($\geq 50\text{K}$), this model predicts $\Delta E_g(T) \propto \exp(-\Theta_B/T)$, but, in most cases $\Delta E_g(T) \propto T^2$ is observed experimentally, (iii) it has been shown that this relation cannot describe the experimental data of $E_g(T)$ even in GaAs³³. Fig.3(b) and 4(b) show the comparison of experimental $E_g(T)$ with Viña's relation. We have obtained the value of Θ_B in the range of 400K to 450K and α_B in the range of 0.40meV/K to 0.44meV/K for the samples with electron concentrations of 9.8×10^{16} to $2.7 \times 10^{18} \text{ cm}^{-3}$. There is no doubt that this gives better fitting than Varshni's relation in the high temperature region, but the fitting in the low temperature region is poor.

As mentioned earlier, it can be shown that the contribution of individual phonon mode to the temperature induced BGS is related to average phonon occupation number $\bar{n}(T)$ and electron-phonon spectral function $f(\epsilon)$. Essentially, $E_g(T)$ can be analytically derived from the expression

$$E_g(T) = E_g(0) - \int d\epsilon f(\epsilon) \bar{n}(\epsilon, T) \quad (4)$$

The electron-phonon spectral function $f(\epsilon)$ is not known *a priori* and extremely complicated to calculate from the first principle. The other option is to use different approximate function for $f(\epsilon)$ to derive temperature dependence of BGS. It has been emphasized conclusively^{24,25} that the indispensable prerequisite for estimation of different parameters obtained from the experimentally measured $E_g(T)$ is the application of an analytical model that accounts for phonon energy dispersion. The BGS results from the superposition of contributions made by phonons with largely different energies, beginning from the zero-energy limit for acoustical phonons up to the cut-off energy for the optical phonons. The basic features of phonon dispersion δ_{ph} and the relative weight of their contributions to $E_g(T)$, may vary significantly from one material to the other. The curvature of the nonlinear part of the $E_g(T)$ is closely related to the actual position of the center of gravity, $\bar{\epsilon}(\epsilon = \hbar\omega)$, and the effective width $\Delta\epsilon$, of the relevant spectrum of phonon modes that make substantial contribution to $E_g(T)$ and this has been quantified by phonon-dispersion co-efficient $\delta_{ph} (= \frac{\Delta\epsilon}{\bar{\epsilon}})$. It has been shown²⁶ that above two empirical models (Eqn.2 and Eqn.3) represent the limiting regimes of either extremely large ($\delta_{ph} \approx 1$) in case of Varshni's relation or extremely small ($\delta_{ph} \approx 0$) in case of Viña's relation. Both these models contradict physical reality for most semiconductors, whose phonon dispersion co-efficient vary between 0.3 to 0.6²⁶. Several analytical models have been presented using different forms of the spectral function $f(\epsilon)$.

Pässler²⁴ has proposed the most successful model, which takes power-law type spectral function, $f(\epsilon) = \nu \frac{\alpha_p}{k_B} \left(\frac{\epsilon}{\epsilon_0}\right)^\nu$ and the cut-off energy ϵ_0 , which is given by $\epsilon_0 = \frac{\nu+1}{\nu} k_B \Theta_p$. Here, ν represents an empirical exponent whose magnitude can be estimated by fitting the experimental data $E_g(T)$. Inserting, the spectral function $f(\epsilon)$ and cut-off energy ϵ_0 into the general equation for band gap shrinkage(Eqn.4), Pässler²⁴ obtained an analytical expression for $E_g(T)$, given by

$$E_g(T) = E_g(0) - \frac{\alpha_p \Theta_p}{2} \left[\sqrt[p]{1 + \left(\frac{2T}{\Theta_p}\right)^p} - 1 \right] \quad (5)$$

where $p=\nu+1$ and α_p is the $T \rightarrow \infty$ limit of the slope $dE_g(T)/dT$, Θ_p is comparable with the average phonon temperature²⁴, $\Theta_p \approx \bar{\epsilon}/k_B$, and the exponent p is related to the material-specific phonon dispersion co-efficient δ_{ph} , by the relation $\delta_{ph} \approx 1/\sqrt{p^2 - 1}$. Depending on the value of δ_{ph} , there are regimes of large and small dispersion which are approximately represented within this model by exponents $p < 2$ and $p \geq 3.3$ respectively. Fig.3(c) and 4(c) show the comparison of experimental $E_g(T)$ with Eqn.5. We obtain an excellent fit to the experimental data. The value of α_p obtained here is in the range of 0.50meV/K to 0.54meV/K and the value of Θ_p in the range of 500 K to 510 K for the samples with electron concentrations of 9.8×10^{16} to $2.7 \times 10^{18} \text{ cm}^{-3}$. The value of the exponent p which is related to the material specific degree of phonon dispersion is obtained between 2.50 to 2.65 for different GaN samples. The value of p obtained here lies in the intermediate dispersion regime and the value of the ratio Θ_p/Θ_D is 0.58, which means that the center of gravity of the relevant electron-phonon interaction are located within the upperhalf of the relevant phonon spectra^{22,23}.

Fig.5 shows how the total redshift $\Delta E_g = E_g(10K) - E_g(320K)$ and the phonon dispersion co-efficient δ_{ph} change with electron concentration. We have observed that ΔE_g , which is the net change of E_g due to the temperature induced BGS, decreases with increase of electron concentration. This has been explained as the screening of the electron-phonon interaction which causes temperature induced BGS by background electrons. When the electron concentration is high, ΔE_g will be less as compared to the case when electron concentration is low. Now the similar effect will also be reflected in the E_g vs. T curves. At lower electron concentration, the curvature of the nonlinear part of the $E_g(T)$ will be more. Hence the value of the exponent p which is obtained from fitting our experimental data will vary with electron concentration. The value of p which controls the curvature of the nonlinear part of the $E_g(T)$ will be less at lower electron concentration and will increase at higher electron concentrations. Now, as mentioned earlier, p is inversely related to δ_{ph} , by the relation $\delta_{ph} \approx 1/\sqrt{p^2 - 1}$. Hence the value of δ_{ph} will decrease as electron concentration increases. The inset of Fig.5 shows this.

In conclusion, BGS has been studied in GaN as a function of electron concentration and temperature. The band-to-band transition shows a redshift due to band-gap narrowing as the electron concentration increases. It has been found that exchange and correlation among majority and minority carriers causes band-gap narrowing in moderately doped n-type GaN. We have also measured the temperature induced band gap reduction in GaN using PL spectroscopy. The importance of electron-phonon interaction on the band gap shrinkage has been established. It has been found that phonon-dispersion based semi-empirical relation is required to explain the experimental data. Screening of electron-phonon interaction is responsible for decrease of temperature induced BGS in samples with higher electron concentration.

The authors thank Professor J. H. Edgar of Kansas State University, for providing some of the samples used in this investigation, and for helpful discussions and encouragement. This work was partly supported by Council of Scientific and Industrial Research, India.

-
- ¹ S. Nakamura and G. Fasol, *The Blue Laser Diode: GaN Based Light Emitters and Lasers*, Springer, New York, 1997.
 - ² R. A. Abram, C. J. Rees and B. L. Wilson, *Adv. Phys.* **27**, 799 (1998).
 - ³ G. D. Mahan, *J. Appl. Phys.* **51**, 2634 (1980).
 - ⁴ H. S. Bennett and J. R. Lowney, *J. Appl. Phys.* **52**, 5633 (1981).
 - ⁵ B. E. Sernelius, *Phys. Rev. B*, **33**, 8582 (1986).
 - ⁶ C. Persson, B. E. Sernelius, A. Ferreira da Silva, C. M. Araujo, R. Ahuja, and B. Johansson, *J. Appl. Phys.* **92**, 3207 (2002).
 - ⁷ E. F. Schubert, I. D. Geopfert and W. Grieshaber, *Appl. Phys. Lett.* **71**, 921 (1997).
 - ⁸ M. Smith, J. Y. Lin, H. X. Jiang and M. Asif Khan, *Appl. Phys. Lett.* **71**, 635 (1997).
 - ⁹ X. Zhang, S. J. Chua, W. Liu and K. B. Chong, *Appl. Phys. Lett.* **72**, 1890 (1998).
 - ¹⁰ E. Iliopoulos, D. Doppalapudi, H. M. Ng and T. D. Moustakas, *Appl. Phys. Lett.* **73**, 375 (1998).
 - ¹¹ M. Yoshikawa, M. Kunzer, J. Wagner, H. Obloh, P. Schlotter, R. Schmidt, N. Herres, and U. Kaufmann, *J. Appl. Phys.* **86**, 4400 (1999).

- ¹² I. H. Lee, J. J. Lee, P. Kung, F. J. Sanchez and M. Razeghi, *Appl. Phys. Lett.* **74**, 102 (1999).
- ¹³ S. Ghosh, *Phys. Rev. B* **62**, 8053 (2000).
- ¹⁴ W. Shan, T. J. Schmidt, X. H. Yang, S. J. Hwang and J. J. Song, *Appl. Phys. Lett.* **66**, 985 (1995).
- ¹⁵ M. O. Manasreh, *Phys. Rev. B*, **53**, 16425 (1996).
- ¹⁶ K. P. Korona, A. Wysmoek, K. Pakua, R. Stepniewski, J. M. Baranowski, I. Grzegory, B. Lucznik, M. Wroblewski, and S. Porowski, *Appl. Phys. Lett.* **69**, 788 (1996).
- ¹⁷ G. D. Chen, M. Smith, J. Y. Lin, H. X. Jang, A. Salvador, B. N. Sverdlov, A. Botchkarov and H. Morkov, *Appl. Phys. Lett.* **79**, 2675 (1996).
- ¹⁸ C. F. Li, Y. S. Huang, L. Malikova and F. H. Pollak, *Phys. Rev. B*, **55**, 9251 (1997).
- ¹⁹ K. B. Nam, J. Li, J. Y. Lin and H. X. Jiang, *Appl. Phys. Lett.* **85**, 3489 (2004).
- ²⁰ Y. P. Varshni, *Physica*, **34**, 149 (1967).
- ²¹ L. Viña, S. Logothetidis and M. Cardona, *Phys. Rev. B* **30**, 1979 (1984).
- ²² J. C. Nipko, C. K. Loong, C. M. Balkas and R. F. Davis, *Appl. Phys. Lett.* **73**, 34 (1998).
- ²³ T. Ruf, J. Serrano, M. Cardona, P. Pavone, M. Pabst, M. Krisch, M. D. Astuto, T. Suski, I. Grzegory and M. Leszczynski, *Phys. Rev. Lett.* **86**, 906 (2001).
- ²⁴ R. Pässler, *Phys. Status Solidi B* **216**, 975 (1999).
- ²⁵ R. Pässler, *Phys. Rev. B* **66**, 085201 (2002).
- ²⁶ R. Pässler, *J. Appl. Phys.* **88**, 2570 (2000); **89**, 6235 (2001); **90**, 3956 (2001).
- ²⁷ Y. Kim, S. G. Subramanya, H. Siegle, J. Krüger, P. Perlin, E. R. Weber, S. Ruvimov and Z. L. Weber, *J. Appl. Phys.* **88**, 6032 (2000).
- ²⁸ E. C. Piquette, P. M. Bridger, R. A. Beach and T. C. McGill, *MRS Internet J. Nitride Semi.* **4S1**, G3.77 (1999).
- ²⁹ S. Dhar and S. Ghosh, *Appl. Phys. Lett.* **80**, 4519 (2002).
- ³⁰ G. D. Chen, M. Smith, J. Y. Lin, H. X. Jiang, S. H. Wei, M. A. Khan and C. J. Sun, *Appl. Phys. Lett.* **68**, 2784 (1996).
- ³¹ D. Volm, K. Oettinger, T. Streibl, D. Kovalev, M. Ben-Chorin, J. Diener, B. K. Meyer, J. Majewski, L. Eckey, A. Hoffmann, H. Amano, I. Akasaki, K. Hiramatsu and T. Detchprohm, *Phys. Rev. B*, **53**, 16543 (1996).
- ³² K. F. Berggren and B. E. Sernelius, *Phys. Rev. B*, **24**, 1971 (1981).
- ³³ E. Grilli, M. Guzzi, R. Zamboni and R. Pavese, *Phys. Rev. B*, **45**, 1638 (1992).
- ³⁴ P. Lautenschlager, M. Garriga, S. Logothetidis and M. Cardona, *Phys. Rev. B*, **35**, 9174 (1987).

Figure Captions

Figure 1. PL spectra of GaN with different electron concentrations at 300 K. An increase of the doping level shifts the band-to-band peak to lower energies. PL spectra are shifted up for clarity. PL spectrum of GaN with $3.8 \times 10^{17} \text{cm}^{-3}$ electron concentration at 10 K is shown in the inset.

Figure 2. Band-gap energy determined from the PL spectra shown as a function of logarithm of electron concentration. Solid lines are the fitted curves to the Eqn.1.

Figure 3. Temperature dependence of the peak positions of band-edge excitonic transition in GaN sample with electron concentration of $3.8 \times 10^{17} \text{cm}^{-3}$. Solid lines are fit to experimental data with (a) Eqn.2, (b) Eqn.3 and (c) Eqn.5.

Figure 4. Temperature dependence of the peak positions of band-edge excitonic transition in GaN sample with electron concentration of $1.3 \times 10^{18} \text{cm}^{-3}$. Solid lines are fit to experimental data with (a) Eqn.2, (b) Eqn.3 and (c) Eqn.5.

Figure 5. Electron concentration dependence of BGS, $\Delta E_g = E_g(10K) - E_g(320K)$. Inset shows how the phonon-dispersion parameter δ_{ph} derived from relation $\delta_{ph} = 1/\sqrt{p^2 - 1}$ changes with electron concentration n . Solid lines are guide for eyes.

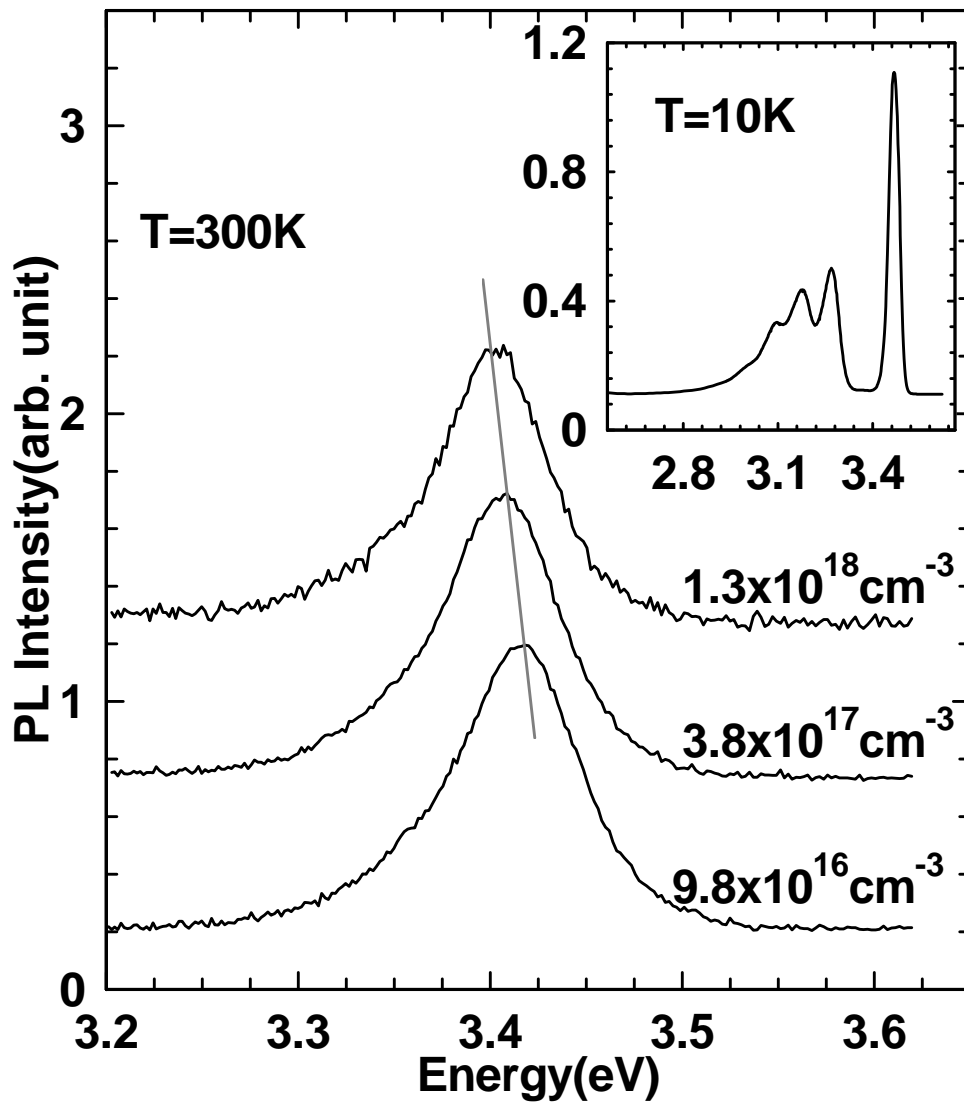


Figure 1

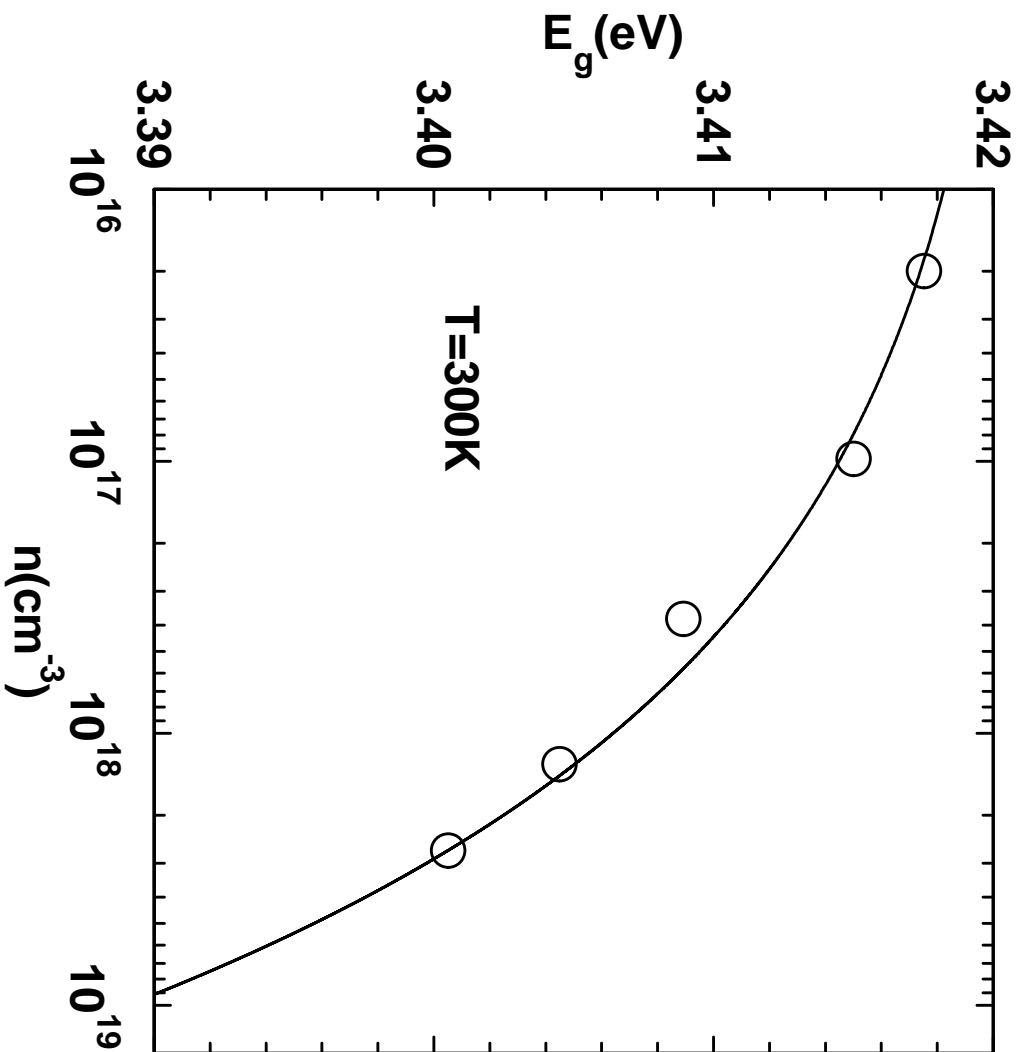


Figure 2

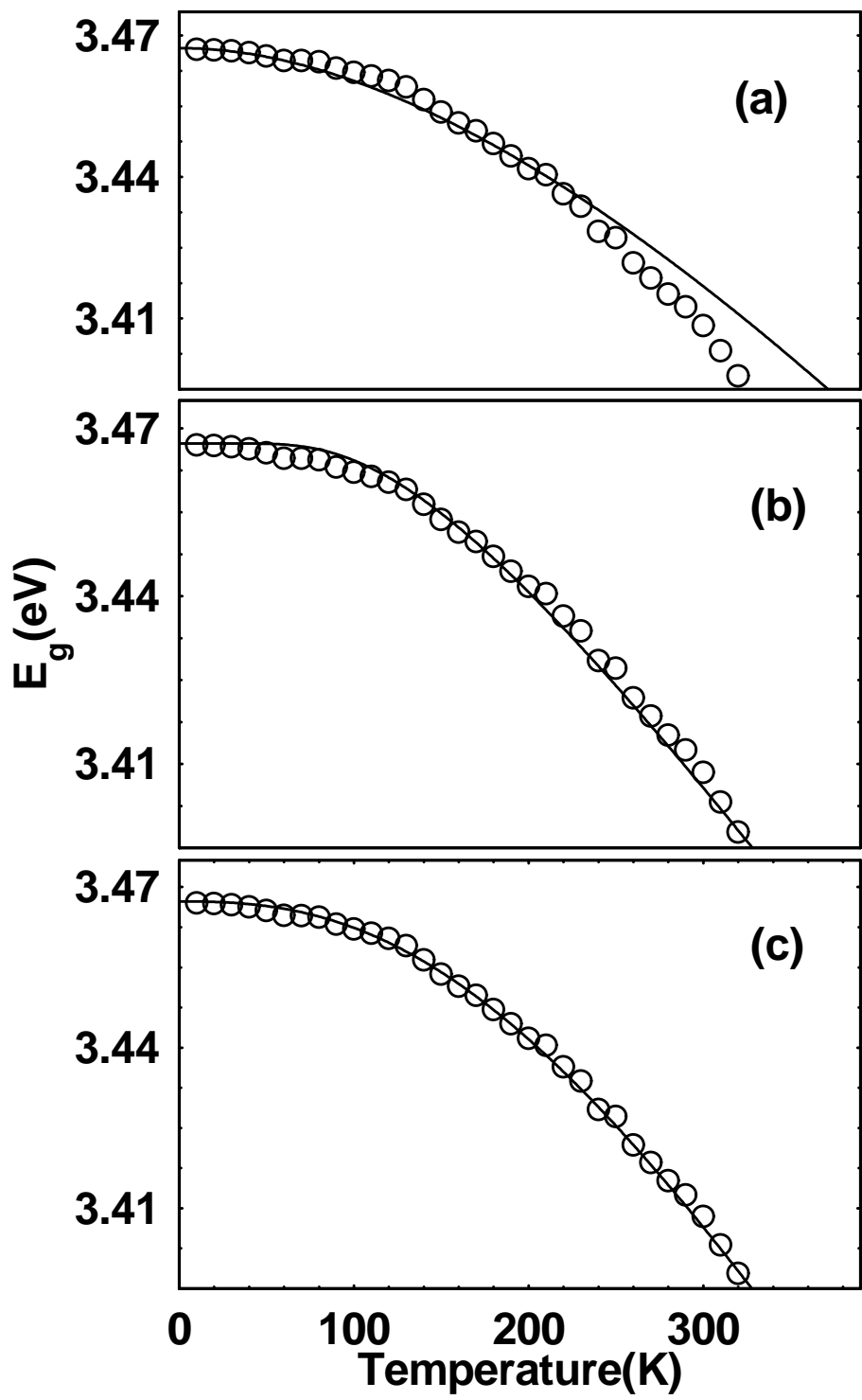


Figure 3

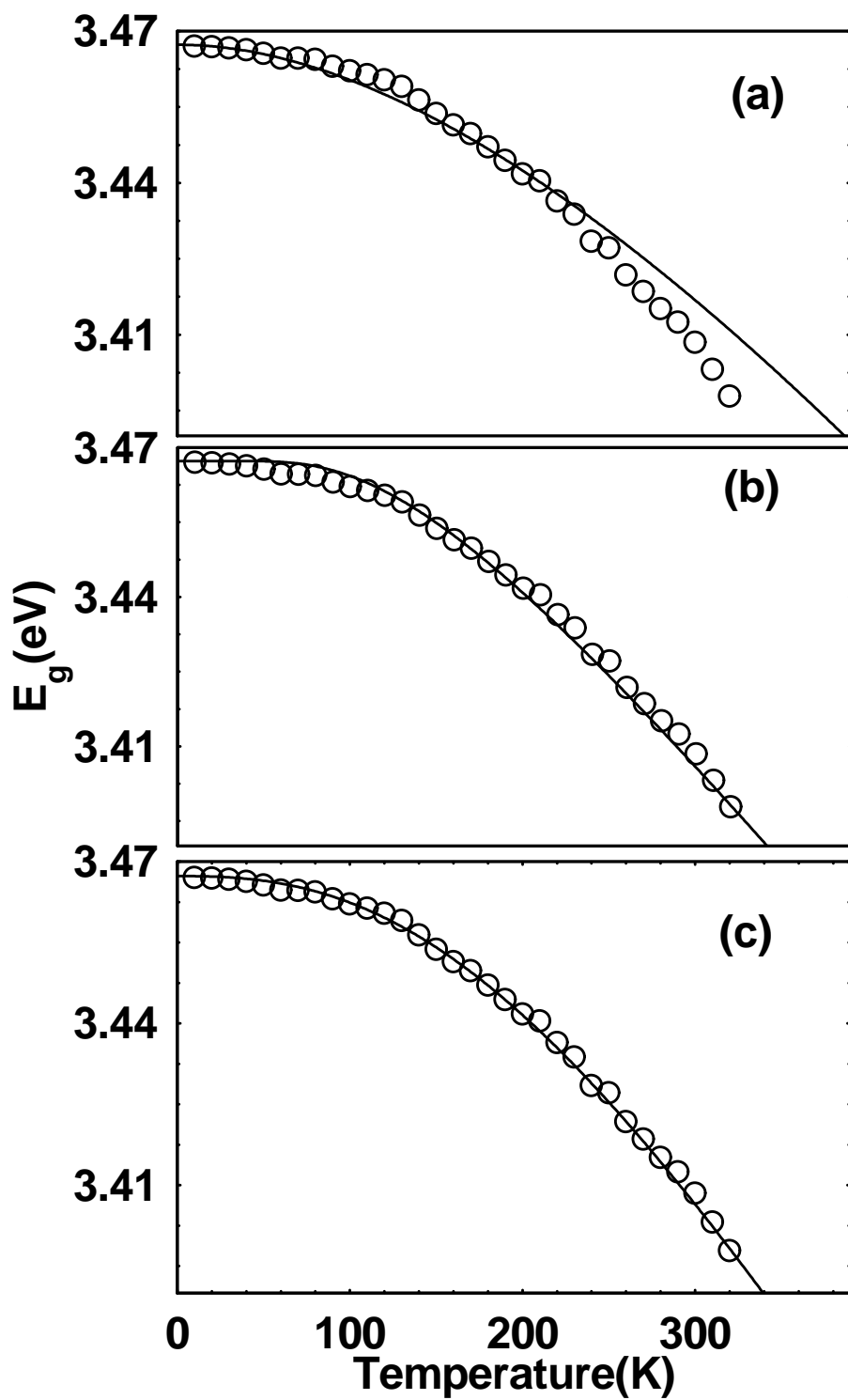


Figure 4

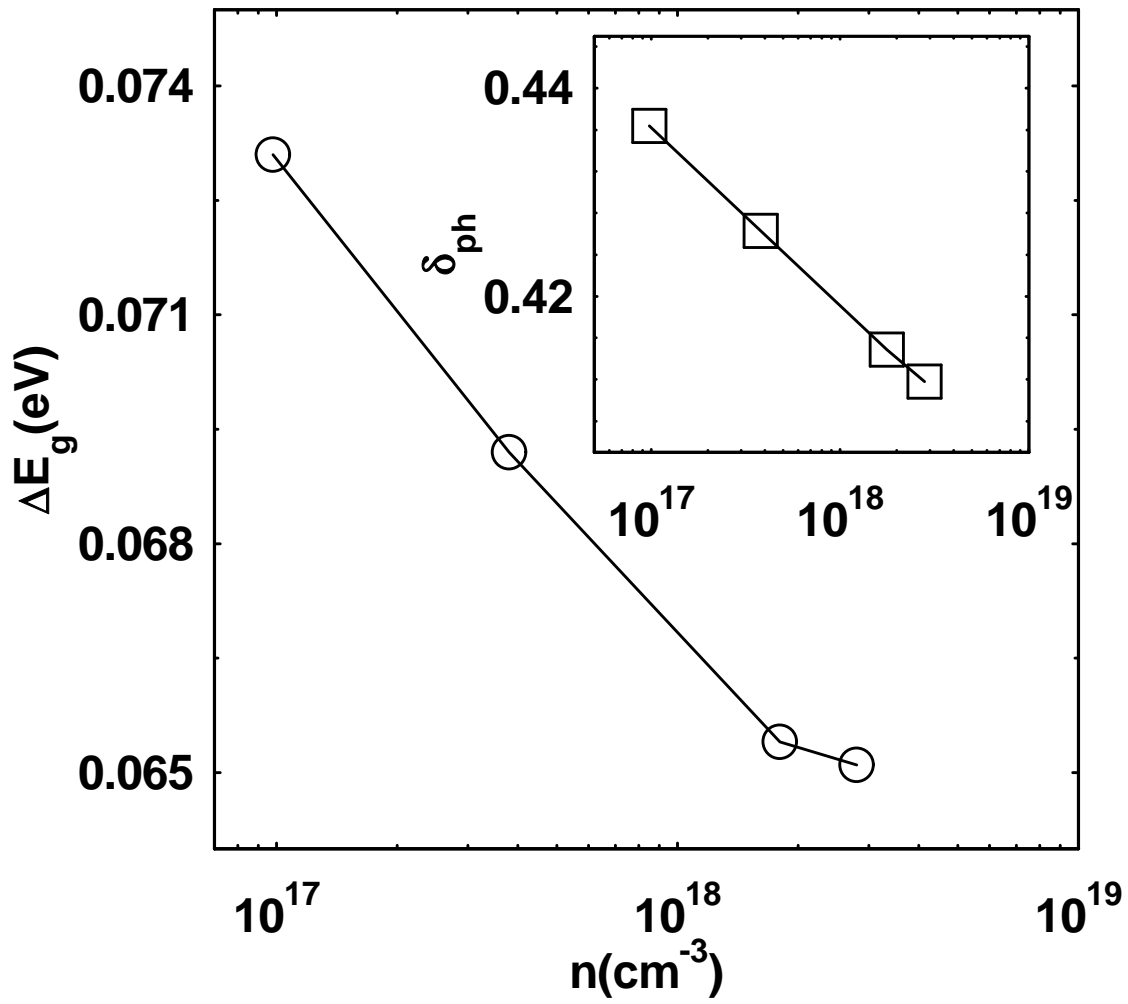


Figure 5